Nonlinear dynamics of system oscillations modeled by a forced Van der Pol generalized oscillator

A. V. Monwanou, L. A. Hinvi, C. H. Miwadinou, J. B. Chabi Orou

Abstract— **This paper considers the oscillations of system modeled by a forced Van der Pol generalized oscillator. These oscillations are described by a nonlinear differential equation. The amplitudes of the forced harmonic, primary resonance super-harmonic and sub-harmonic oscillatory states are obtained using the harmonic balance technique and the multiple time scales methods. Hysteresis and jump phenomena in the system oscillations are obtained. Bifurcation sequences displayed by the model for each type of oscillatory states are performed numerically through the fourth-order Runge-Kutta scheme.**

Index Terms— **forced Van der Pol generalized oscillator, harmonic balance technique, resonant states, hysteresis, bifurcation.**

I. INTRODUCTION

The theory of oscillators has shown that many dynamics phenomena can be modeled by oscillators in engineering, biochemistry, biophysics, and communications. Nonlinear oscillations and its applications in physics, chemistry, engineering, are studied with some analytical, numerical and experimental methods. The most interesting nonlinear oscillators are self-excited and the study of their dynamics is often difficult. Duffing, Van der Pol and Rayleigh oscillators have been studied by many researchers. Nowadays, much research has accomplished the composition of these oscillators. Multiresonance, chaotic behavior and its control, bifurcations, limit cycle stability, hysteresis and jump phenomena, analytic solutions, plasma oscillations, noise effect... are seriously analyzed. Many problems in physics, chemistry, biology, etc., are related to nonlinear self-excited oscillators [1]. Thus, Balthazar Van der Pol (1889-1959) was a Dutch electrical engineer who initiated modern experimental dynamics in the laboratory. He, first, introduced his (now famous) equation in order to describe triode oscillations in electrical circuits in 1927 [2]. The mathematical model for the system is a well-known second order ordinary differential equation with cubic nonlinearity. Since then thousands of papers have been published achieving better approximations to the solutions occurring in such nonlinear systems. The Van der Pol oscillator is a classical example of self-oscillatory system and is now considered as very useful mathematical model that can be used in much more complicated and modified systems. But, why this equation is so important to mathematicians, physicists and engineers and is still being extensively studied?

During the first half of the twentieth century, Balthazar Van der Pol pioneered fields of radio and telecommunications [2]. In an era when these areas were much less advanced than they are today, vacuum tubes were used to control the how of electricity in the circuitry of transmitters and receivers. Contemporary with Lorenz, Thompson, and Appleton, Van der Pol, in 1927, experimented with oscillations in a vacuum tube triode circuit and concluded that all initial conditions converged to the same periodic orbit of finite amplitude. Since this behavior is different from the behavior of solutions of linear equations, Van der Pol proposed a nonlinear differential equation

$$\ddot{x} + x - \epsilon(1 - x^2)\dot{x} = 0 \tag{1}$$

commonly referred to as the (unforced) Van der Pol equation [3], as a model for the behavior observed in the experiment. In studying the case $\epsilon \gg 1$, Van der Pol discovered the importance of what has become known as relaxation oscillations (Van der Pol[4]). Van der Pol went on to propose a version of (1) that includes a periodic forcing term:

$$\ddot{x} + x - \epsilon(1 - x^2)\dot{x} = E \sin \Omega\, t. \tag{2}$$

Many systems have characteristics of two types of oscillators and whose equation presents a combination of terms of these oscillators. Thus, we have the systems characterized by Van der Pol and Rayleigh oscillators namely the Van der Pol generalized oscillator or hybrid Van der pol-Rayleigh oscillator modeled by

$$\ddot{x} + x - \epsilon(1 - ax^2 - b\dot{x}^2)\dot{x} = 0 \tag{3}$$

The Van der Pol generalized oscillator as all oscillator, models many physical systems. Thus, we have [5] who models a bipedal robot commotion with this oscillator known as Hybrid Van der Pol-Rayleigh oscillators". In the present paper, we considered the forced Van der Pol generalized oscillator

$$\ddot{x} + x - \epsilon(1 - ax^2 - b\dot{x}^2)\dot{x} = E \sin \Omega\, t \tag{4}$$

where a, b are positives cubic nonlinearities, $\epsilon \ll 1$ is damping parameters while E and Ω stand for the amplitude and the pulsation of the external excitation. We focuss our attention on the equation of motion, the resonant states, the chaotic behavior. The effects of differents parameters in general are found.

A.V. Monwanou, Institut de mathématiques et de Sciences Physiques de Dangbo, Université d'Abomey-Calavi, Bénin, Tél : 0022997124274.

L. A. Hinvi, Institut Universitaire de Technologie de Lokossa, Université Nationale des Sciences, Technologies, Ingénieurie et Mathématiques d'Abomey, Tél : 0022996855897.

C. H. Miwadinou, Ecole Normale Supérieure de Natitingou Université Nationale des Sciences, Technologies, Ingénieurie et Mathématiques d'Abomey, Tél : 0022997934189.

J. B. Chabi Orou, Institut de mathématiques et de Sciences Physiques de Dangbo, Université d'Abomey-Calavi, Bénin, Tél : 0022997471847

The paper is organized as follows: Section 2 gives an analytical treatment of equation of motion. Amplitude of the forced harmonic oscillatory states is obtained with harmonic-balance method. Section 3 investigate using multiple time-scales method, the resonant cases. The stability conditions are found by the perturbation method. Section 4 evaluates bifurcation and chaotic behavior. The conclusion is presented in the last section.

II. Amplitude of the Forced Harmonic Oscillatory States

Assuming that the fundamental component of the solution and the external excitation has the same period, the amplitude of harmonic oscillations can be tackled using the harmonic balance method. For this purpose, we express its solutions as

$$x = A\sin(\Omega\, t + \xi), \quad (5)$$

$$(1-\Omega^2)A\sin(\Omega\, t) + \xi + \epsilon\left[(1-a\xi^2)A\Omega - \frac{aA^3\Omega}{4} - \frac{3bA^3\Omega^3}{4}\right]\cos\Omega\, t + \epsilon\left(\frac{aA^3\Omega - 3bA^3\Omega^3}{4}\right)\cos 3\Omega\, t - \epsilon a\xi A^2\sin 2\Omega\, t = E\sin\Omega\, t. \quad (6)$$

By equating the constants and the coefficients of $\sin$ and $\cos$, we have

$$\begin{cases} (1-\Omega^2)A = E, & (7) \\ \xi = 0, & (8) \\ \epsilon\left[(1-a\xi^2)A\Omega - \dfrac{aA^3\Omega}{4} - \dfrac{3bA^3\Omega^3}{4}\right] = 0. & (9) \end{cases}$$

$$\begin{cases} (1-\Omega^2)^2A^2 = E^2, & (10) \\ \epsilon^2\left[(1-a\xi^2)A\Omega - \dfrac{aA^3\Omega}{4} - \dfrac{3bA^3\Omega^3}{4}\right]^2 = 0. & (11) \end{cases}$$

Equations (10 -11) lead to

$$[(1-\Omega^2)^2 - \epsilon^2\Omega^2]A^2 + \frac{\epsilon^2\Omega^2}{2}(a+3b\Omega^2)A^4 - \frac{\epsilon^2\Omega^2}{16}(a+3b\Omega^2)^2A^6 = E^2 \quad (12).$$

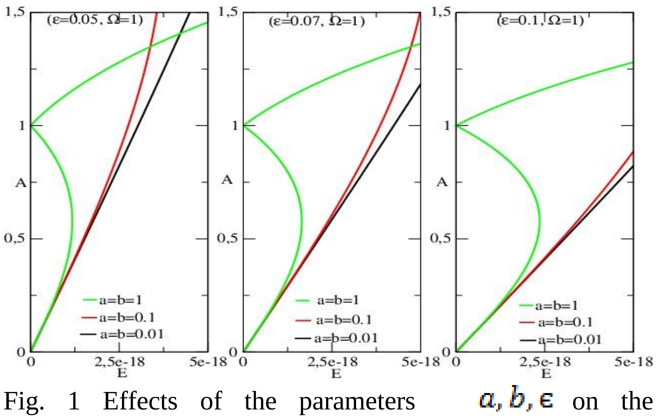

Fig. 1 Effects of the parameters a, b, ϵ on the amplitude-response curves with $\Omega = 1$.

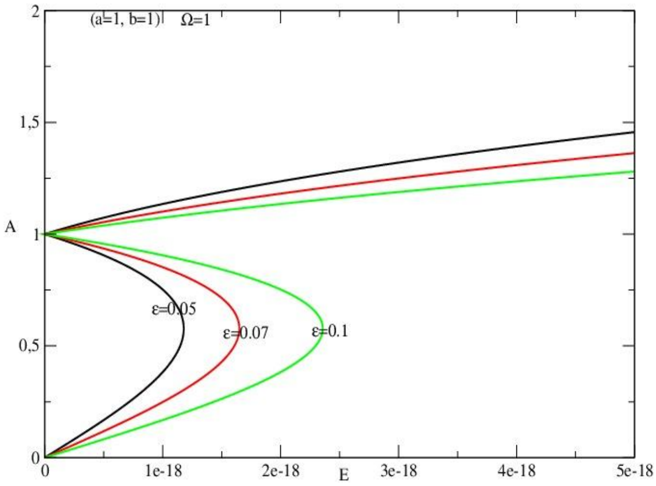

Fig.2 Effects of the parameter ϵ on the amplitude-response curves with $a = 1, b = 1, \Omega = 1$.

The figures 1 and 2 show the effects of the parameters a, b, ϵ on the amplitude- response curves. Through these figures, we note that for small value of Rayleigh coefficient a and Van der Pol coefficient b the amplitude-response is linear and when its increase, the hystereris and jump phenomenas appear. The gape of jump phenomenon decreases when the damping parameter ϵ increases but hysteresis and jump phenomena persist.

III. Resonant States

We investigate the different resonances with the multiple time scales method MSM. In such a situation, an approximate solution is generally sought as follows:

$$x(t,\epsilon) = x_0(T_0, T_1) + \epsilon x_1(T_0, T_1) \;.... \quad (13)$$

With $T_n = \epsilon^n t$

The derivatives operators can now be rewritten as follows:

$$\begin{cases} \dfrac{d}{dt} = D_0 + \epsilon D_1 \\ \dfrac{d^2}{dt^2} = D_0^{\,2} + 2\epsilon D_0 D_1 \end{cases} \quad (14)$$

Where

$$D_n^m = \frac{\partial^m}{\partial\, T_n^{\,m}}.$$

A. Primary resonant

In this state, we put that $E \approx \epsilon\tilde{E}$. The closeness between both internal and externalfrequencies is given by $\Omega = 1 + \epsilon\sigma$ where $\sigma = 0(1)$ o(1) is the detuning parameter, the internal frequency is 1. Inserting (13) and (14) into (4) we obtain:

$$(D_0^{\,2} + 2\epsilon D_0 D_1)(x_0 + \epsilon x_1) + x_0 + \epsilon x_1 - \epsilon\left(1 - a(x_0+\epsilon x_1)^2 - b[(D_0+\epsilon D_1)(x_0+\epsilon x_1)]^2\right)(D_0 + \epsilon D_1)(x_0+\epsilon x_1) = E\sin\Omega\, t. \quad (15)$$

Equating the coefficients of like powers of ϵ after some algebraic manipulations, we obtain:

$$\begin{cases} D_0{}^2 x_0 + x_0 = 0, \\ D_1{}^2 x_1 + x_1 = E \sin \Omega\, t - 2 D_1 D_0 x_0 - \\ \epsilon(1 - a x_0{}^2 - b\,(D_0\, x_0)^2)(D_0\, x_0). \end{cases} \quad (16)$$

The general solution of the first equation of system (16) is

$$x_0(T_0, T_1) = A(T_1) Exp(j T_0) + CC, \qquad (17)$$

where CC represents the complex conjugate of the previous terms. $A(T_1)$ is a complex function to be determined from solvability or secular conditions of the second equation of system (16). Thus, substituting the solution x_0 in (16) leads us to the following secular criterion

$$D_1{}^2 x_1 + x_1 = j[-2A' - (1 - a|A|^2 - 3b|A|^2)A]e^{jT_0} + (b-a)A^3 e^{3jT_0} - \frac{jE}{2} e^{j(1+\epsilon\sigma)t} + CC \ (18)$$

$$D_1{}^2 x_1 + x_1 = j\left[-2A' - (1 - (a-3b)|A|^2)A - \frac{E}{2} e^{j(\epsilon\sigma)t}\right]e^{jT_0} + (b-a)A^3 e^{3jT_0} + CC. (19)$$

The secular criterion follows

$$\left[-2A' - (1 - (a-3b)|A|^2)A - \frac{E}{2} e^{jT_1}\right] = 0. \ (19)$$

In polar coordinates, the solution of (19) is

$$A(T_1) = \frac{1}{2}\, p(T_1) e^{j\theta(T_1)} + CC \ \ (20).$$

Where p and θ are real quantities and stand respectively for the amplitude and phase of oscillations. After injecting (20) into (19), we obtain

$$-p' - j\theta' p + \frac{1}{2} p + \frac{(a+3b)p^3}{8} - \frac{jE}{2} e^{j(\sigma T_1 - \theta(T_1))} = 0, (21)$$

We separate real and imaginary terms and obtain the following coupled flow for the amplitude and phase:

$$\begin{cases} -p' + \frac{1}{2} p - \frac{(a+3b)p^3}{8} = \frac{E \cos \phi}{2} \\ -\phi' p + p\sigma = \frac{E \sin \phi}{2}, \end{cases} \qquad (22)$$

where the prime denotes the derivative with respect to T_1 and $\phi = \sigma T_1 - \theta(T_1)$. For the steady-state conditions ($\phi' = p' = 0 \Leftrightarrow p_0 = \phi_0 = 0$), the following nonlinear algebraic equation is obtained:

$$\frac{1 + 4\sigma^2}{4} p_0^2 - \frac{a+3b}{8} p_0^4 + \frac{a+3b}{64} p_0^6 = \frac{E^2}{4} \ (23)$$

Where p_0 and ϕ_0 are respectively the values of p and ϕ in the steady-state. Eq.(23) is the equation of primary resonance flow. Now, we study the stability of the process, we assume that each equilibrium state is submitted to a small perturbation as follows

$$\begin{cases} p = p_0 + p_1 \\ \phi = \phi_0 + \phi_1. \end{cases} (24)$$

Where p_1 and ϕ_1 are slight variations. Inserting (24) into (22) and canceling nonlinear terms, we obtain

$$-p_1' = -\frac{1}{2}\left[1 + 3\frac{(a+3b)p_0{}^2}{4}\right] p_1 - p_0 \sigma \phi_1, (25)$$

$$\phi'_1 = \frac{\sigma p_1}{p_0} - \frac{1}{2}\left[1 - \frac{(a+3b)p_0{}^2}{4}\right]\phi_1, \qquad (26)$$

The stability process depends on the sign of eigenvalues Γ of the equations (25) and (26). The eigenvalues are given through the following characteristic equation

$$\Gamma^2 + 2Q\Gamma + R = 0, (27)$$

where

$$\begin{cases} Q = \frac{1}{2}\left[1 + \frac{(a+3b)p_0{}^2}{4}\right] \\ R = \frac{1}{4}\left[1 + 3\frac{(a+3b)p_0{}^2}{4}\right]\left[1 - \frac{(a+3b)p_0{}^2}{4}\right] - \sigma^2 \end{cases}$$

Since $Q > 0$, the steady-state solutions are stable if $R > 0$ and unstableotherwise.

Figures 3 and 4 display the primary resonance curves obtained from (23) for different values of the parameters a, b, E. Linear resonances curves are obtained shown the increasing of the resonance amplitude when the external forced amplitude increase. We found also the peak value of resonance amplitude is higher when $a + 3b > 1$ than the case $a + 3b < 1$.

Figure 5 displays the amplitudes response curves obtained from (23) for different values of the parameters, b and σ. We obtained that for $a + 3b \ll 1$, the amplitude-response is a linear function of E and the slope decreases as σ increases. The hystereris phenomena appears when $a + 3b$ is important for small value of σ and disappears when σ increases.

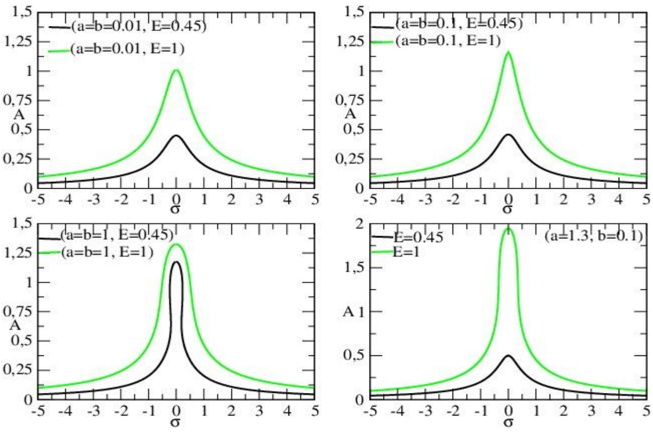

Fig. 3 Effects of the parameters a, b, E on primary resonance curves.

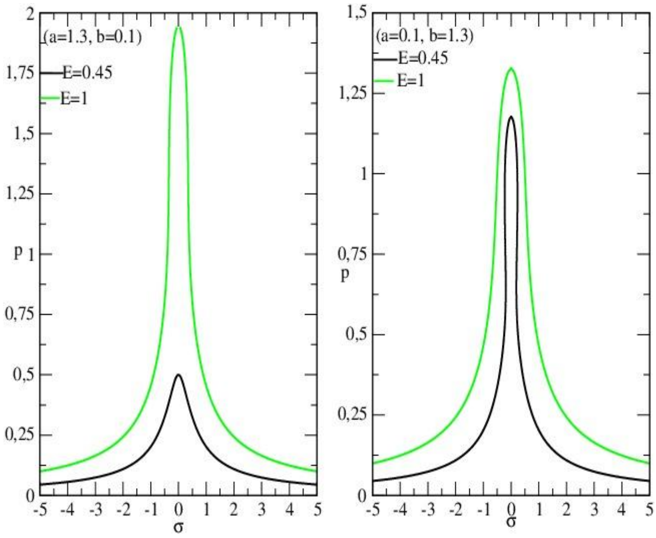

Fig. 4 Effects of the parameters a, b, E on the primary resonance curves.

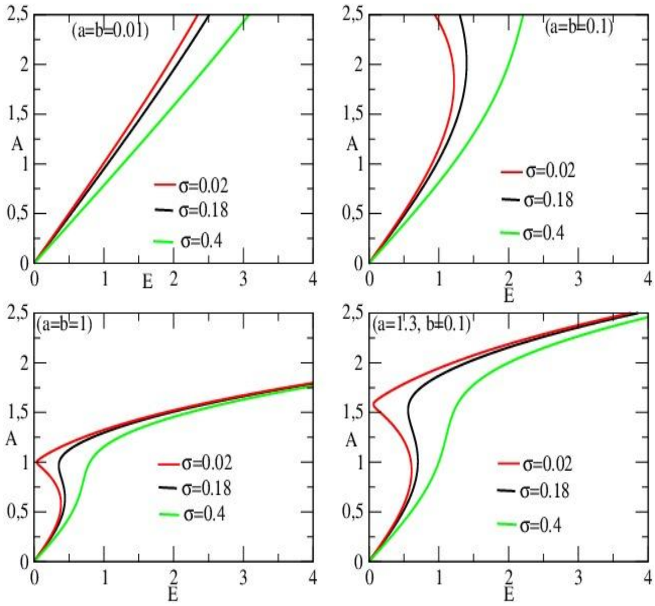

Fig. 5 Effects of the parameters a, b, σ on the amplitude-response curves.

A. Superharmonic and subharmonic oscillations

When the amplitude of the sinusoidal external force is large, other type of oscillations can be displayed by the model, namely the superharmonic and the subharmonic oscillatory states. It is now assumed that $E \approx \epsilon^0 \tilde{E}$ and therefore, one obtains the following equations at different order of ϵ.

In order ϵ^0,

$$D_0{}^2 x_0 + x_0 = E \sin \Omega\, t, \quad (28)$$

In order ϵ

$$D_1{}^2 x_1 + x_1 = -2D_1 D_0 x_0 - \epsilon\left(1 - a x_0{}^2 - b\,(D_0\, x_0)^2\right)(D_0\, x_0). \quad (29)$$

The general solution of Eq.(29) is

$$\begin{cases} x_0 = A(T_1)e^{jT_0} + \Lambda e^{j\Omega T_0} \\ \Lambda = \dfrac{E}{2(1-\Omega^2)} \end{cases} \quad (30)$$

Substituting the general solution x_0 into Eq. (29), after some algebraic manipulations, we obtain

$$D_1{}^2 x_1 + x_1 = j[-2A' + (1-(a+3b)|A|^2) - 2A\Lambda^2(a+3b\Omega^2)]e^{jT_0}$$
$$[\Omega\Lambda - 2(a+3b)|A|^2\ \Omega - (a+3b)\Omega\Lambda^3]e^{j\Omega T_0} + j(b-a)A^3 e^{3jT_0} + j\Omega\Lambda^3(b\Omega^2 - a)e^{3j\Omega T_0} + j[-a(2+\Omega) + 3b\Omega^2]A\Lambda^2 e^{j(1+2\Omega)T_0} + j[-a(2+\Omega) + 3b\Omega]A^2\Lambda e^{j(2+\Omega)T_0} + j[a(2-\Omega) + 3b\Omega]\bar{A}^2\,\Lambda e^{j(2-\Omega)T_0} + j[a(2\Omega-1) + 3b\Omega]\,A\Lambda^2 e^{j(1-2\Omega)T_0} + CC$$
(31)

where CC represents the complex conjugate of the previous terms. From Eq.(31), it comes that superharmonic and subharmonic states can be found from the quadratic and cubic nonlinearities. For the cases of superharmonic oscillation we consider $3\Omega = 1 + \epsilon\sigma$, while the subharmonic oscillation to be treated is $\Omega = 3 + \epsilon\sigma$.

B1 Superharmonic states

For the first superharmonic states $3\Omega = 1 + \epsilon\sigma$, equating resonant terms at 0 from Eq.(31), we obtain:

$$[-2A' + A[1-(a+3b)|A|^2 - 2\Lambda^2(A + 3b\Omega^2)] + \Lambda^3\Omega(b\Omega^2 - a)e^{j\epsilon\sigma T_0}] = 0 \quad (32)$$
.

Using (20) and after some algebraic manipulations, we re-write (32) as follows

$$\begin{cases} p' = \dfrac{p}{2}\left[1 + \dfrac{(a+3b)p^2}{4} - 2\phi^2(A + 3b\Omega^2)\right] + \Lambda^3\Omega(b\Omega^2 - a)\phi, \\ p\phi' = p\sigma - \Lambda^3\Omega(b\Omega^2 - a)\sin\phi \end{cases} \quad (33)$$

With $\phi = \sigma T_1 - \boldsymbol{\theta}$.

The amplitude of oscillations of this superharmonic states ($\phi' = p' = 0 \Leftrightarrow p_0 = \phi_0 = 0$) is governed by the following nonlinear algebraic equation

$$\frac{(a+3b)^2}{64}p_0^6 - \mu\frac{a+3b}{4}p_0^4 + (\mu^2 + \sigma^2)p_0^2 + \Lambda^6\Omega^2(a - b\Omega^2)^2 = 0$$
(34)

With $\mu = \frac{1}{2} - \Lambda^2(a + 3b\Omega^2)^2$

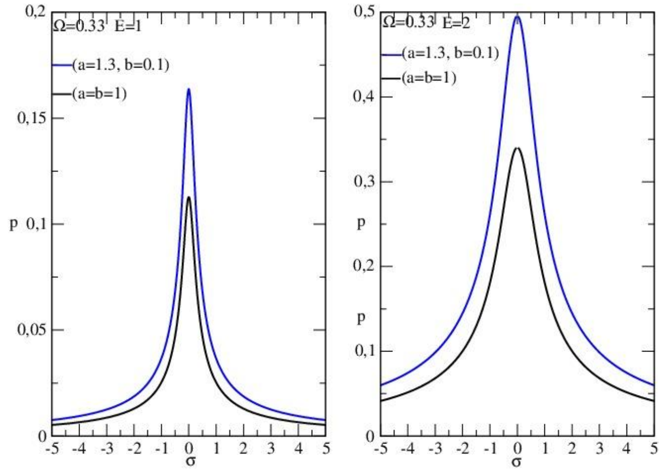

Fig. 6 Effects of the parameters a, b, E on the superharmonic resonance curves.

From figure (6), we note that in superharmonic states, the resonance curve is linear and the amplitude increases as the external force amplitude E increases. We note also that this amplitude decreases as $a + 3b$ increases.

B2.Subharmonic states

For the first subhamonic states $\Omega = 3 + \epsilon\sigma$ equating resonant terms at 0 from Eq.(31), we obtain:

$$[-2A' + A[1 - (a+3b)|A|^2 - 2\Lambda^2(A + 3b\Omega^2)] + [a(2-\Omega) + 3b\Omega]\bar{A}^2\Lambda e^{j\epsilon\sigma T_0}] = 0 \quad (35)$$

.

Using (20) and after some algebraic manipulations, we rewrite (35) as follows

$$\begin{cases} p' = \frac{p}{2}\left[1 - \frac{(a+3b)p^2}{4} - 2\Lambda^2(A + 3b\Omega^2)\right] + [a(2-\Omega) + 3b\Omega]\frac{\Omega\, p^2}{4}\cos\varphi\,, \\ \frac{p\varphi'}{3} - \frac{p\sigma}{3} = [a(2-\Omega) + 3b\Omega]\frac{\Omega\, p^2}{4}\sin\varphi \end{cases} \quad (36)$$

with
$\varphi = \sigma T_1 - 3\boldsymbol{\theta}$.

The amplitude of oscillations of this subharmonic states ($\varphi' = p' = 0 \Leftrightarrow p_0 = \varphi_0 = 0$) is governed by the following nonlinear algebraic equation.

$$\frac{(a+3b)^2}{64}p_0^4 - [4\mu(a+3b) + \Lambda^2[a(2-\Omega) + 3b\Omega]\frac{p_0^2}{16} + \left(\mu^2 + \frac{\sigma^2}{9}\right)p_0^2 = 0, \quad (37)$$

with $\mu = \frac{1}{2} - \Lambda^2(a + 3b\Omega^2)^2$.

Figure (7) shows the order 3 subharmonic resonance curve with effects of parameters a and b and external excitation. Each of this parameter affected the stable resonance amplitude domain. It can be seen noticed that amplitude and frequency resonance increase with amplitude of external excitation.

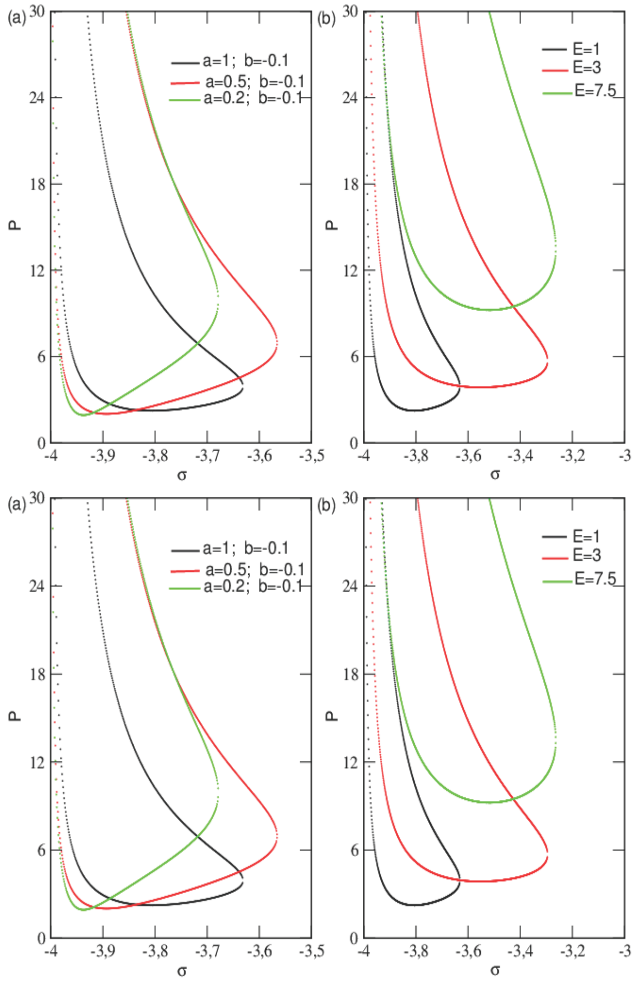

Fig.7 (a): Effects of the parameters a and b on subharmonic resonance with $E = 1$; (b) : Effect of external excitation E on subharmonic resonance curves with $a = 1, b = 1$.

IV. Bifurcation and Chaotic Behavior

The aim of this section is to find some bifurcation structures in the nonlinear dynamics of forced Van der Pol generalized oscillator described by equation (4) for resonant states since they are in interest for the system. For this purpose, we numerically solve this equation using the fourth-order Runge Kutta algorithm (Piskunov[8]) and plot the resulting bifurcation diagrams and the variation of the corresponding largest Lyapunov exponent as the amplitude E, the parameters of nonlinearity a, b varied. The stroboscopic time period used to map various transitions which appear in the model is $T = \frac{2\pi}{\Omega}$.

The largest Lyapunov exponent which is used here as the instrument to measure the rate of chaos in the system is defined as

$$lyn = \lim_{t \to \infty} \frac{\ln\sqrt{dx^2 + d\dot{x}^2}}{t}, \qquad (38)$$

Where dx and $d\dot{x}$ are respectively the variations of x and $\dot{x}$. Initial condition that we used in the simulations of this section is $(x_0, \dot{x}_0)$=(1,1). For the set of parameters

$$a = \{1,6\},\ b = \{1,6\}, E = \{1,6\}, \epsilon = \{0.01,10\}, \Omega = \{1; \tfrac{1}{3}; 3\}$$

, the bifurcation and Lyapunov exponents diagrams for primary, superharmonic and subharmonic resonances are plotted respectively in Figs. (8), (9) and ((10), (11)). The bifurcation diagrams are in upper frame and its corresponding Lyapunov exponents are in lower frame. From the diagrams, it is found that the model can switch from periodic to quasi-periodic, non periodic and chaotic oscillations. Since the model is highly sensitive to the initial conditions, it can leave a quasi-periodic state for a chaotic state without changing the physical parameters. Therefore, its basin of attraction has been plotted (see Figs.(16), (17)) in order to situate some regions of the initial conditions for which chaotic oscillations are observed. From these figures, we conclude that chaos is more abundant in the subharmonic resonant states than in the superharmonic and primary resonances. This confirms what has been obtained through their bifurcation diagrams and Lyapunov exponent.
We noticed that for the small value of ε, the system is not chaotic.
In order to illustrate such situations, we have represented the various phase portraits using the parameters of the bifurcation diagram for which periodic, quasi periodic and non periodic oscillations motions are observed in Figs. (12), (13), (14) and chaotic motions are observed in Fig.(15) for the two values of the parameters a, b, E above. From the phases diagram we observed appearance of the closed curve and the torus that confirm the two precedent types of motions predicted and the linear types of resonances seen in the third section.

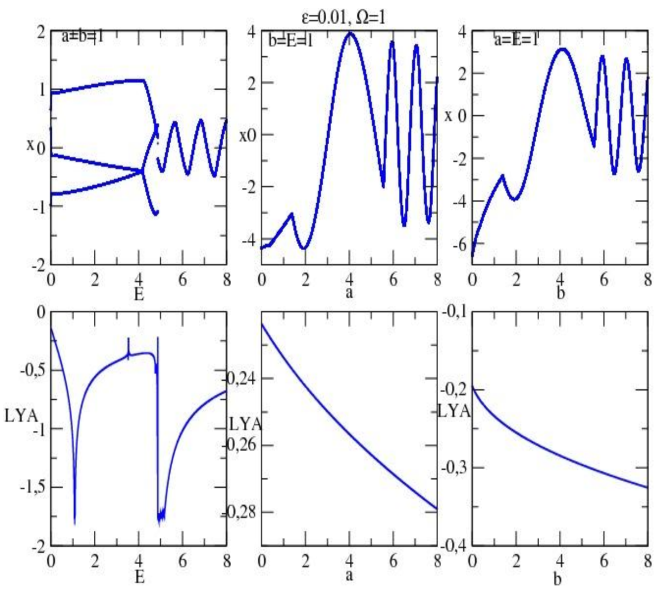

Fig. 8 Bifurcation diagram (upper frame) and Lyapunov exponent (lower frame) for $\epsilon = 0.01, \Omega = 1$ in primary resonance case.

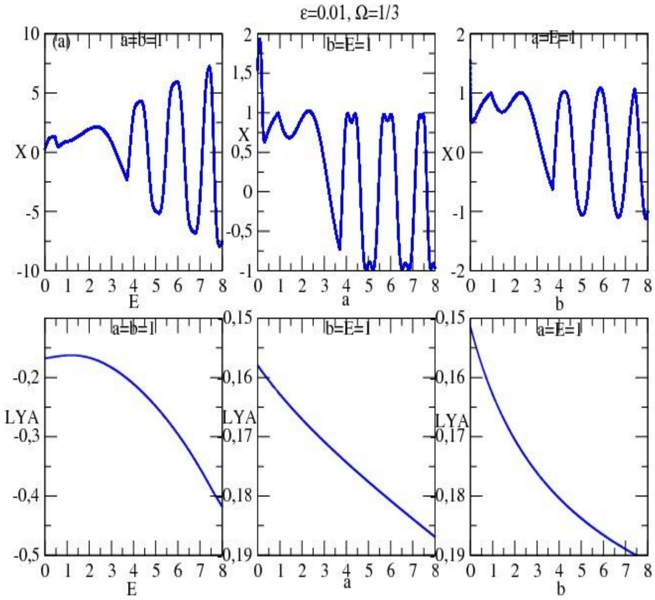

Fig. 9 Bifurcation diagram (upper frame) and Lyapunov exponent (lower frame) for $\epsilon = 0.01, \Omega = \frac{1}{3}$ in superharmonic case.

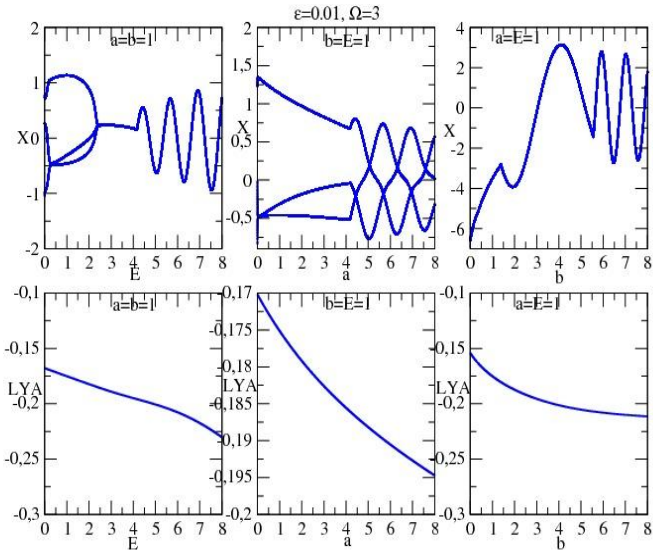

Fig. 10 Bifurcation diagram (upper frame) and Lyapunov exponent (lower frame) for $\epsilon = 0.01, \Omega = 3$ subharmonic case.

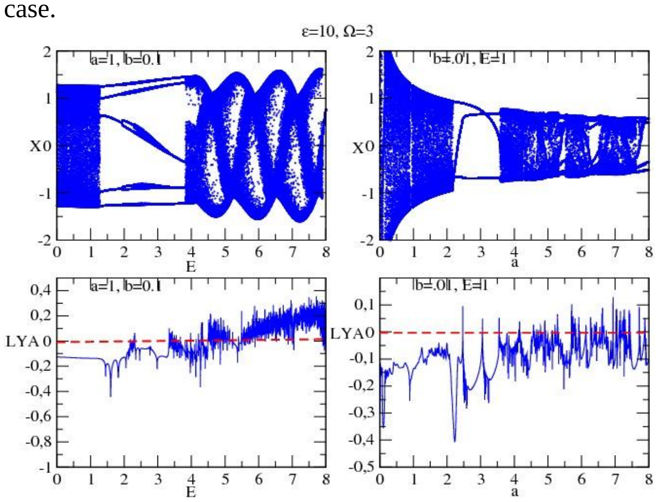

Fig. 11 Bifurcation diagram (upper frame) and Lyapunov exponent (lower frame) for, $\epsilon = 10,\ \Omega = 3$, Subharmonic states case.

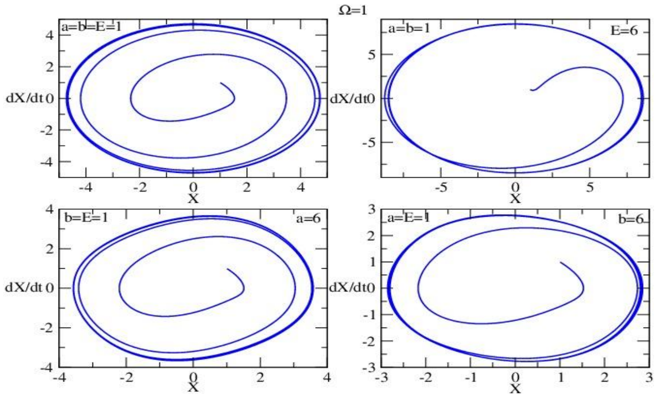

Fig. 12 Phases diagram for parameters values in figure, $\epsilon = 0.01$, primary resonance case.

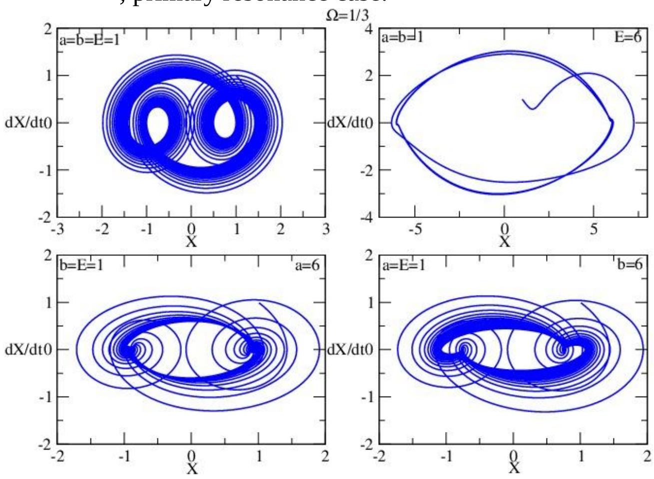

Fig. 13 Phases diagram for parameters values in figure, $\epsilon = 0.01$, Superharmonic states case.

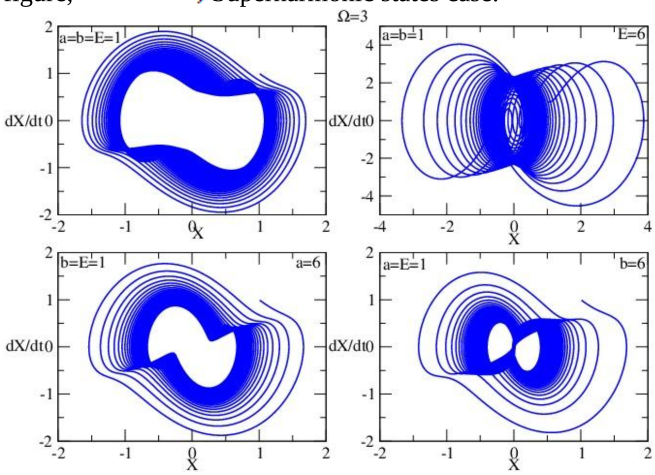

Fig. 14 Phases diagram for parameters values in figure ,$\epsilon = 0.01$, Subharmonic states case.

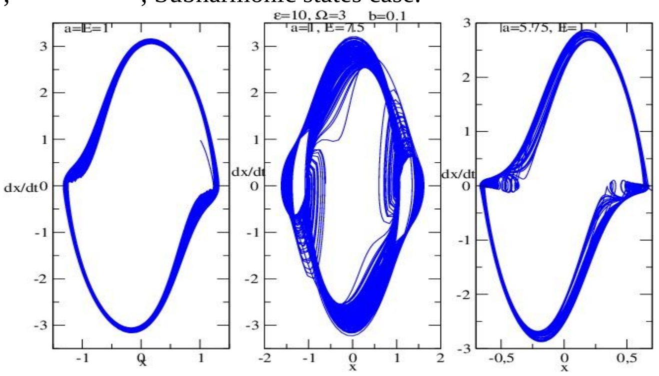

Fig. 15 Phases diagram for parameters values in figure, ,$\epsilon = 10, \Omega = 3$.

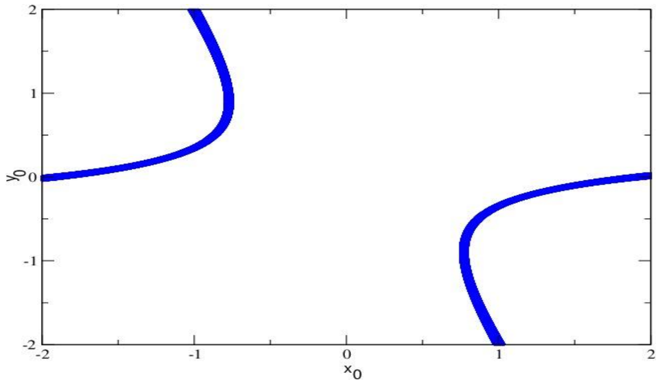

Fig. 16 Chaoticity basin for parameters values in figure 9 with$E = 1$.

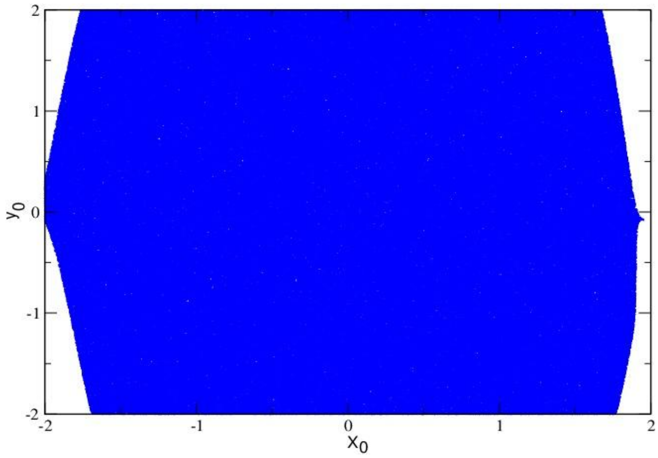

Fig. 17 Chaoticity basin for parameters values in figure 11 with$E = 7.5$.

IV. Conclusion

In this work, we have studied the nonlinear dynamics of system oscillations modeled by forced Van der Pol generalizedoscillator. In the harmonic case, the balance method has enabled us to derive the amplitude of harmonic oscillations, and the effects of the different parameters on the behaviors of model have been analyzed. For the resonant states case, the response amplitude, stability (for primary resonance case) have been derived by using multiple time-scales method and perturbation method. It appears the first-orders superharmonic and subharmonic resonances.

The effects of different parameters on these resonances are been found and we noticed that the Van der Pol, Rayleigh parameters and the external force amplitude have several action on the amplitude reponse and the resonances curves. The influences of these parameters on the resonant, hysteresis and jump phenomena have been highlighted. Our analytical results have been confirmed by numerical simulation. Various bifurcation structures showing different types of transitions from quasi-periodic motions to periodic and the beginning of chaotic motions have been drawn and the influences of different parameters on these motions have been study. It is noticed that behaviors of system have been controlled by the parameters a, b, E and but also the damping parameter ϵ. We conclude that chaos is more abundant in the subharmonic resonant states than in the superharmonic and primary resonances. This confirms what has been obtained through their bifurcation diagrams and Lyapunov exponent. The results show a way to predict admissible values of the signal amplitude for a corresponding set of parameters. This could be helpful for the experimentalists who are interested in trying to stabilize such a system with external forcing. For practical interests, it is useful to develop tools and to find ways to control or suppress such undesirable regions. This will be also useful to control high amplitude of oscillations obtained and which are generally source of instability in physics system.

ACKNOWLEDGMENT

The authors thank very much Drs. Enjieu Kadji, Victor Kamdoum and Peguy Roussel Nwagour for their collaborations. We also thank very much the anonymous referees whose useful criticisms, comments and suggestions would helped strengthen the content and the quality of the paper.

REFERENCES

[1] S. Rajasekar, S. Parthasarathy, M. Lakshmanan,''Prediction of horseshoe chaos in BVP and DVP oscillators. Chaos, Solitons and Fractals'', 1992; 2 : 271.
[2] Marios, Tsatsos, ''Theoretical and Numerical Study of the Van der Pol equation(Dissertation)'', 2006.
[3] B. Van der Pol ,''A theory of the amplitude of free and forced triode vibrations'', Radio Review, 1(1920), pp. 701 -710, 754 -762.
[4] B. Van der Pol, ''On Relaxation Oscillations I'', Phil. Mag., 2 1926, pp. 978-992.
[5] A. C de Pina Filho, M. S. Dutra, ''Application of hybrid Van der Pol-Rayleigh oscillators for modeling of a Bipedal robot'', 2009.
[6] C. Hayashi, ''Nonlinear Oscillations in Physical Systems'', (McGraw Hill, New York, 1964, Sec.1:5.
[7] A. H. Nayfeh, (1981), ''Introduction to perturbation techniques'', (John Wiley and Sons,New York, 1981, Sec.4:5.
[8] N. Piskunov, ''Calcul Differentiel et integral'', Tome II, 9e edition, MIR, Moscou 1980.
[9] C.H .Miwadinou, A. V. Monwanou, J. B. Chabi Orou, ''Active control of the parametric resonance in the modified Rayleigh-Duffing oscillator'', African Review of Physics, 2014; 9 : 227 -235.
[10] C.H .Miwadinou, A. V. Monwanou, J. B. Chabi Orou,''Effect of Nonlinear dissipation on the basin boundaries of a driven two-well modified Rayleigh-Duffing oscillator'',Int. J. Bifurcation and Chaos 2015; 25 : 1550024.
[11] C.Ainamon, C. H. Miwadinou, A.V. Monwanou, J. B. Chabi Orou, ''Analysis of Multiresonance and Chaotic Behavior of the Polarization in Materials Modeled by a Duffing Equation with Multifrequency Excitations''. Applied Physics Research 2014; 6 :74 -86.
[12] C. H., Miwadinou, A. L. Hinvi, A. V .Monwanou, J. B. Chabi Orou, ''Nonlinear dynamics of a φ^6 modified Duffing oscillator: resonant oscillations and transition to chaos'',Nonlinear Dyn 2017; 88 : 93 -113.

Biographical Notes

Adjimon Vincent Monwanou received the M.Sc. and Ph.D. degrees in Fluid Dynamics and Nonlinear Dynamics from Université d'Abomey-Calavi, Bénin. His current research mainly covers Nonlinear problem in Physics include stability analysis in Fluid Flows. Dr. Adjimon Vincent Monwanou is author or coauthor of more than 15 research articles published in several prestigious journals.

Laurent Amoussou Hinvi received the M.Sc. and Ph.D. degrees in Fluid Dynamics and Nonlinear Dynamics from Universit_e d'Abomey-Calavi, B_enin. His current research mainly covers Nonlinear problem in Physics include stability analysis in Fluid Flows. Dr. Laurent Amoussou Hinvi is author or coauthor of more than 10 research articles published in several prestigious journals.

Clément Hodévèwan Miwadinou received the M.Sc. and Ph.D. degrees in Fluid Dynamics and Nonlinear Dynamics from Université d'Abomey-Calavi,
Bénin. His current research mainly covers Nonlinear problem in Physics include stability analysis in Fluid Flows. Dr. Clément Hodévèwan Miwadinou is author or
coauthor of more than 10 research articles published in several prestigious journals.

Jean Bio Chabi Orou received the M.Sc. and Ph.D. degrees in Fluid Dynamics and Nonlinear Dynamics from Université d'Abomey-Calavi, Bénin. His current research mainly covers Nonlinear problem in Physics include stability analysis in Fluid Flows. Prof. Jean Bio Chabi is author or coauthor of more than 55 research articles published in several prestigious journals.

.